Journal of Structural Dynamics, 3, (pp. 88-108) 2025
Optimum Tuned Mass Damper Parameters for Complex Structures Subjected to Base-Excitation Using Single-Mode Approximation

Optimum Tuned Mass Damper Parameters for Complex Structures Subjected to Base-Excitation Using Single-Mode Approximation

Shashank Pathak*[1], Frédéric Bourgeois †[2], and Arnaud Deraemaeker ‡[3]

[1] *Assistant Professor, (School of Civil & Environmental Engineering), Indian Institute of Technology Mandi-175005, Mandi, India*
[2] *Professor, (Laboratoire de Mathématiques d'Orsay), Université Paris-Saclay, CNRS- 91405, Orsay, France*
[3] *Professor, (Building Architecture and Town Planning (BATir)), Université libre de Bruxelles, Brussels-1050, Belgium*

Abstract

This paper addresses the problem of optimal tuning of a tuned mass damper (TMD) attached to a complex structure that is dynamically excited by its base. It proposes new analytical formulae which are based on the reduction of the multiple-degree-of-freedom (MDOF) model of the host-structure into an equivalent single-degree-of-freedom (SDOF) model. As it has been recognized in the literature that the traditional single mode approximation used to perform this reduction is not valid for base-excited systems, we propose an improved version that leads to the definition of two mass ratios instead of one in the traditional approach. Taking into account this new mass ratio, the equal peak method is used to derive analytically the optimal values of stiffness and damping of the TMD for a given mass ratio of the device. The introduction of a second mass ratio leads to the existence of two sets of equations for the optimal parameters, depending on the relative values of the two mass ratios. It is shown, however, that only the first set of equations is of practical use. The application of these new tuning rules is illustrated using a MDOF model of a high-rise building. It demonstrates the efficiency of the approach when the first mode of vibration is targeted. When higher modes are of interest, modal interactions are important, which cause a slight to moderate unbalance of the peaks.

Keywords: Equal-peak approach; Analytical solution; Passive vibration control; Tuned mass damper; Multi-degree-of-freedom systems; Single mode approximation

Received on December 11, 2024, Accepted on March 25, 2025, Published on March 31, 2025

1 Introduction

Tuned mass dampers (TMDs) are being installed extensively across the globe on civil infrastructure such as buildings, bridges and footbridges in order to mitigate the effects of dynamic excitations due to wind, earthquake or pedestrians. In order for these devices to be efficient, it is essential to properly tune their frequency and damping to target the mode of interest.

There is a huge literature available on the optimization of TMDs, and several notable reviews have also been published on the topic [1, 2, 3]. The TMD parameters (stiffness and damping) can be optimized in the time domain or in the frequency domain. In most cases, the information of the frequency content of the excitation is available rather than the exact time history. Frequency domain approaches are therefore more useful and popular.

Some popular frequency domain approaches are the equal peak method [4] and the variance minimization method [5]. On the other hand, the energy method [6] and the area ratio method [7] are some popular time-domain approaches. Out of all these methods, the most widely used one is the equal peak method, which is a frequency domain approach and provides simple analytical expressions for the optimal tuning ratio and optimal damping ratio as a function of the chosen mass ratio between the TMD and the host structure.

*shashank@iitmandi.ac.in
†frederic.bourgeois@universite-paris-saclay.fr
‡arnaud.deraemaeker@ulb.be

Although the equal-peak approach does not provide the exact minimization of the H_∞-norm of the frequency response function, it has been shown extensively in previous studies to be a very good approximation for all the practical cases considering undamped host-systems [8]. It was also shown by Ghosh et al. in [9] that this approach, also called the fixed-point theory, works reasonably well even for moderately damped (1-3% damping ratio) host systems. Moreover, analytical expressions can be obtained, including the damping of the host-system, as in [9, 10]. Of course, if the damping in the host-structure is more important, such an approach will fail, but on the other hand, the addition of a TMD to an already heavily damped structure is probably not of much practical interest.

The aforementioned methods provide analytical expressions of the optimal frequency ratio and damping values for the case of a TMD attached to the host system modelled as a simple mass-spring system, which of course limits their applicability to real-life structures where a more complex model is often needed. In [11], the authors have generalized the work of [12] and discussed the idea of optimizing the TMD attached to multi-degree-of-freedom (MDOF) or continuous systems by converting them into an equivalent SDOF system corresponding to a particular mode of interest (usually the dominant/first mode of vibration). This approach, also called the single-mode approximation, is justified by the fact that the TMD has a narrow-band effect around the natural frequency of interest where the response is dominated by the corresponding mode, and assumes that the modes are sufficiently spaced in frequency.

In [13], Warburton demonstrated the applicability of this equivalence approach for a variety of practical cases where the MDOF host system is subjected to harmonic or white-noise excitations, the input force is acting directly on the host-system, and the absolute responses (displacement, velocity, and acceleration) are minimized. The authors could however not demonstrate such an equivalence when the MDOF host system is subjected to a base excitation and relative responses are the target of the optimization.

In their work, it was clearly stated that the analogy to obtain the equivalent SDOF is not applicable for this case. This particular case is however of special importance in earthquake engineering where relative displacement responses are of interest and are the quantity to be minimized using the TMD devices. It is important to highlight the fact that despite the inadequacy of the equivalence approach for base excited structures, it is often used in the literature (see, for example, [14]).

The above literature review shows that simple analytical formulae can be used to obtain the optimal parameters of TMDs only when the MDOF system is subjected to forces on the host-structure and the modes are sufficiently spaced in frequency. In this case, the MDOF host system can be replaced by an SDOF system using the traditional single-mode approximation. When base excitation is applied, this approach, although often used in the literature, is not correct. This is the main motivation for developing a new technique in the present paper.

The paper is organized as follows: in Section 2, the equations of motion for an MDOF host-system excited through its base are established and reduced to an SDOF system using a single-mode approximation. The equation of motion is extended taking into account the addition of the TMD, and the non-dimensional transfer function for the host-system is given as a function of two mass ratios μ and μ_1.

Then in Section 3, based on this transfer function, the equal peak approach is used to derive the analytical formulae for optimal stiffness and damping of the TMD for base-excited systems. Due to the existence of three and not two invariant points for the transfer function for certain values of the set of parameters (μ, μ_1), a discussion is presented on the adequate choice of the two invariant points to be set at equal height. This results in two sets of equations to be used in different regions of the parameter space of (μ, μ_1), and is illustrated by plotting the transfer functions for different values of μ and μ_1.

A practical example of the tuning of a TMD starting from the MDOF model of a high-rise building excited by its base is presented in Section 4 in order to illustrate the improvements of the new formulae compared to the traditional equations derived by Warburton. The paper finishes with conclusions and outlooks in Section 5. The detailed complex calculations for the optimal damping ratio are given in Annex A & B.

2 Single-mode approximation for base-excited systems

As explained in the introduction, single-mode approximation is traditionally used to simplify the dynamics of the host-system and obtain analytical expressions of tuning rules for TMDs. Complex structures typically exhibit a rich dynamic behavior where several of their mode shapes can be excited by external sources. The TMD is an SDOF resonant system which, when coupled to the host structure will only be efficient in a narrow frequency band. Its application is therefore only pertinent if one wishes to increase the damping of the host structure around one chosen resonance frequency, as it will have no effect on the dynamics of the host-system at other frequencies. With this in mind, it becomes pertinent, for the purpose of optimally tuning the TMD, to restrict the dynamics of the complex MDOF system to an equivalent SDOF system where only one mode is retained.

It is important however to understand that proper tuning of the TMD can only be achieved if the above conditions are met. As already stated, if the modal density is high around the mode one wishes to damp, the single-mode approximation cannot be used [11]. This paper focuses on the specific case of base excitation. Because of the nature of this excitation, and as will be shown further in Section 4 , the level of excitation of the modes strongly decreases with the frequency so that in general, only the first mode is dominant in the response. In applications therefore, only the first mode shape typically needs to be damped, so that the use of a TMD is pertinent, even if the frequency content of the excitation (such as earthquakes) extends over a number of mode shapes.

One also needs to understand that the single-mode approximation using the first mode of the structure is relevant for the tuning of the TMD targeted to this specific mode, but that the model is not aimed at representing the full dynamics of the system under random or pseudo-random excitation.

2.1 Equations of motion for a base-excited system using single mode approximation

Consider a complex structure excited by its base (Fig. 1). The discrete equations of motion of the system without the TMD can be obtained using the finite element method giving the mass, damping, and stiffness matrices denoted by $[M]$, $[C]$, and $[K]$, respectively.

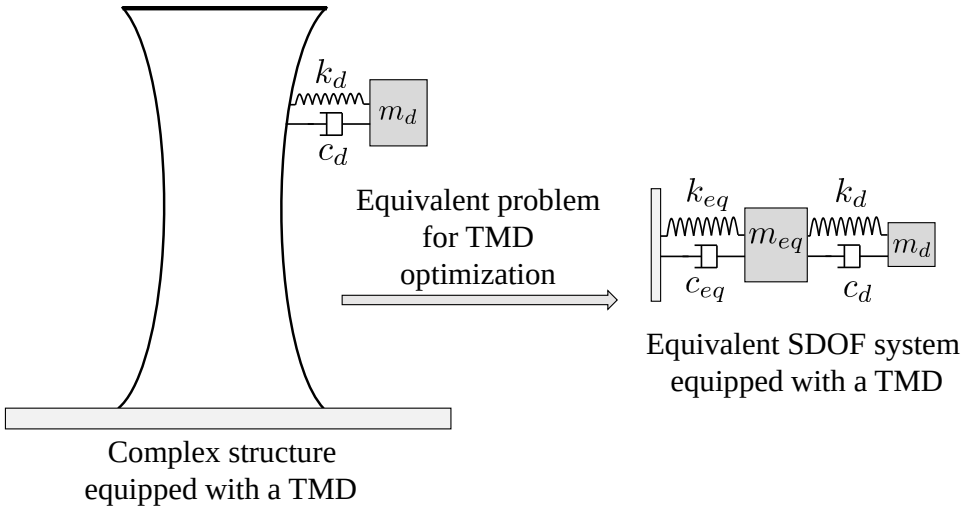

Fig. 1: MDOF system and corresponding equivalent SDOF system equipped with a TMD

In the case of base excitation (e.g., seismic motion), a common approach is to write the equations of motion in terms of relative displacements, which are also the quantities of interest for design. In this case, however, and as highlighted by Warburton in [13], the traditional single-mode approximation cannot be applied, because, as will be demonstrated below, it would lead to an inconsistency in the transfer function to be minimized. The author in [13] did not however propose a solution to this problem, and the aim of this paper is to solve this unresolved issue.

Let the complex structure shown in Fig. 1 be subjected to a horizontal ground acceleration $\ddot{X}_o$. The governing equations of motion can be written as:

$$[M]\{\ddot{X}_r\} + [C]\{\dot{X}_r\} + [K]\{X_r\} = -[M]\{T\}\ddot{X}_o \tag{1}$$

where, $\{X_r\}$ is the $N \times 1$ vector of relative displacements of the system and is equal to $\{X\} - X_o\{T\}$. Here, $\{T\}$ is a Nx1 vector with ones at the DOFs corresponding to the imposed displacement (location and direction) and zeros everywhere else. The equivalent force vector $-[M]\{T\}\ddot{X}_o$ represents the base-excitation. Projection in the modal basis leads to a set of decoupled equations of the type

$$\eta_i\ddot{z}_{ri} + 2\xi_i\eta_i\omega_i\dot{z}_{ri} + \eta_i\omega_i^2 z_{ri} = -\{\psi_i\}^T[M]\{T\}\ddot{X}_o \tag{2}$$

where η_i is the modal mass of the i^{th} mode ($\eta_i = \{\psi_i\}^T[M]\{\psi_i\}$, where $\{\psi_i\}$ is i^{th} mode shape vector), ξ_i and ω_i are the modal damping ratio and natural angular frequency of the i^{th} mode.

As discussed in the introduction of Section 2, it is pertinent to only retain the mode to which the TMD will be tuned, if there are no other modes which are close in frequency. For the sake of generality and although we stated that in practice only the first mode is of interest for base-excited systems, we restrict the equations of motion to the i^{th} mode. The relative displacement response at the k^{th} DOF when only the i^{th} mode is retained is then $x_{rik} = z_{ri}(t)\psi_{ik}$, where ψ_{ik} represents the amplitude of the i^{th} mode shape at the k^{th} DOF.

Thus, substituting $z_{ri} = x_{rik}/\psi_{ik}$ in Eq. 2 leads to

$$m_{eq}\ddot{x}_{rik} + c_{eq}\dot{x}_{rik} + k_{eq}x_{rik} = -\tilde{m}_{eq}\ddot{X}_o \tag{3}$$

where,

$$m_{eq} = \eta_i/\psi_{ik}^2 \tag{4}$$
$$k_{eq} = \eta_i\omega_i^2/\psi_{ik}^2 \tag{5}$$
$$c_{eq} = 2\eta_i\xi_i\omega_i/\psi_{ik}^2 \tag{6}$$

which are traditionally obtained with the single-mode approximation, and

$$\tilde{m}_{eq} = \left(\{\psi_i\}^T[M]\{T\}\right)/\psi_{ik} \tag{7}$$

We note that Eq. 3 differs from the equation of motion of an SDOF system excited by the base, for which the excitation term would be $-m_{eq}\ddot{X}_o$ and for which analytical expressions have been established in [13], for the optimal tuning of TMDs considering base motion and relative displacements (case 5 in [13]).

This inconsistency, preventing the use of these analytical formulae for general MDOF systems using the single-mode approximation in the case of base excitation, was already identified in [13] where it was shown that in order to use the analogy, one would need to have $m_{eq} = \tilde{m}_{eq}$ (Eqs. (35) and (36) in Appendix III of [13]), which is most often not the case for general MDOF systems. We propose hereafter, instead of trying using the analogy, to develop new tuning rules taking into account the fact that $m_{eq} \neq \tilde{m}_{eq}$.

If a TMD is attached to the system at the k^{th} DOF to alleviate the response in the i^{th} mode of vibration, it introduces an additional term $f_d = \{\psi_i\}^T\{F_d\}/\psi_{ik}$ in the equation of motion where F_d is the force due to the TMD in physical coordinates.

The equation of motion becomes

$$m_{eq}\ddot{x}_{rik} + c_{eq}\dot{x}_{rik} + k_{eq}x_{rik} = -\tilde{m}_{eq}\ddot{X}_o + f_d \tag{8}$$

Eq. 8 shows that on the contrary to the case where the host-system is a mass-spring system, the masses on the left and right of the equality sign are different. In addition to the traditional mass ratio $\mu = m_d/m_{eq}$ (where m_d is the mass of the TMD), we need to introduce a second mass ratio $\mu_1 = \tilde{m}_{eq}/m_{eq}$. It is clear that in the determination of optimal TMD parameters (stiffness k_d and damping c_d), these two mass-ratios will play a crucial role.

In summary, the process of reducing the MDOF host system to an SDOF system for base excitation shows that the masses on the left and right of the equality sign may be different in the resulting SDOF equation. As of now, there is no analytical solution in the literature to find the optimal parameters for such a system with two different mass ratios. The next sections are therefore devoted to the derivation of such optimal parameters as a function of μ and μ_1.

2.2 Dimensionless transfer function

The method we propose to apply to find the optimal parameters of the TMD when the host-system is a complex structure under base excitation is the equal peak method, which is generally derived based on the equations of motion

written in the frequency domain. It is a common practice to write these equations in a dimensionless form before applying the method in order to obtain general formulae which do not depend on specific parameters of the model. The transfer function resulting from Eq. 8 is therefore derived in its non-dimensional form in the frequency domain below.

The equations of motion of the equivalent SDOF host-system with a TMD attached are given by Eq. 9 and reduce to Eq. 10 in the frequency domain.

$$\begin{bmatrix} m_{eq} & 0 \\ 0 & m_d \end{bmatrix} \begin{Bmatrix} \ddot{x}_{rik} \\ \ddot{x}_{rd} \end{Bmatrix} + \begin{bmatrix} c_{eq}+c_d & -c_d \\ -c_d & c_d \end{bmatrix} \begin{Bmatrix} \dot{x}_{rik} \\ \dot{x}_{rd} \end{Bmatrix} + \begin{bmatrix} k_{eq}+k_d & -k_d \\ -k_d & k_d \end{bmatrix} \begin{Bmatrix} x_{rik} \\ x_{rd} \end{Bmatrix} = -\begin{bmatrix} \tilde{m}_{eq} & 0 \\ 0 & m_d \end{bmatrix} \begin{Bmatrix} 1 \\ 1 \end{Bmatrix} \ddot{X}_o \tag{9}$$

$$\begin{bmatrix} -\omega^2 m_{eq} + j\omega(c_{eq}+c_d) + k_{eq} + k_d & -j\omega c_d - k_d \\ -j\omega c_d - k_d & -\omega^2 m_d + j\omega c_d + k_d \end{bmatrix} \begin{Bmatrix} X_{rik}(\omega) \\ X_{rd}(\omega) \end{Bmatrix} = \omega^2 \begin{Bmatrix} \tilde{m}_{eq} \\ m_d \end{Bmatrix} X_o(\omega) \tag{10}$$

x_{rd} is the relative displacement of the TMD with respect to the imposed base displacement, j is the imaginary number.

The transfer function $h_{ed}(\omega)$, giving the ratio of the relative displacement of the host-structure at the location of the TMD and the imposed acceleration at the base (including the TMD) can be written as:

$$h_{ed}(\omega) = \frac{X_{rik}(\omega)}{\omega^2 X_o(\omega)} = \frac{\tilde{m}_{eq}(-m_d\omega^2 + k_d + j\omega c_d) + m_d(k_d + j\omega c_d)}{(-m_d\omega^2 + k_d + j\omega c_d)(-\omega^2 m_{eq} + k_d + k_{eq} + j\omega(c_{eq}+c_d)) - (k_d + j\omega c_d)^2} \tag{11}$$

Now, using the two mass-ratios (μ and μ_1), frequency ratio ($f = \omega_d/\omega_n$, where $\omega_d = \sqrt{k_d/m_d}$ and $\omega_n = \sqrt{k_{eq}/m_{eq}}$), damping ratio ($r = c_d/(2m_d\omega_d)$), and assuming that the host-system is lightly damped ($c_{eq} \approx 0$), Eq. 11 leads to the dimensionless transfer function $H_{ed}(g)$ as a function of the normalized frequency ($g = \omega/\omega_n$):

$$H_{ed}(g) = \omega_n^2 h_{ed}(\omega) = \frac{\mu f^2 + \mu_1(f^2 - g^2) + 2jgfr(\mu + \mu_1)}{(1-g^2)(f^2-g^2) - \mu g^2 f^2 - 2jgfr(g^2 - 1 + \mu g^2)} \tag{12}$$

To obtain the optimal TMD parameters f and r, the approach consists in minimizing some norm of $H_{ed}(g)$. The more common approaches are to minimize the H_∞ or the $H2$-norm. The later is best suited when the excitation is a random noise, and its aim is to minimize the variance of the output quantity of interest (here the relative displacement), while the former is aimed at minimizing the maximum of the transfer function for harmonic excitation. It is important to understand that real excitations, such as seismic activity are neither a pure random noise, nor an harmonic excitation. As input spectra for earthquakes vary with the region considered in the world, as well as the type of soil, analytical solutions are difficult to generalize.

The authors understand that the choice made in this paper to work with the H_∞-norm is debatable, so that one has to understand the optimality of the parameters only in the sense of the norm considered, and with the idea in mind that the aim here is to decrease the amplitude of the main resonant mode, for which an H_∞ approach, leading to equal peaks of reduced amplitude, is judged appropriate. The approach we follow is therefore to minimize the maximum of $Y = |H_{ed}(g)|$:

$$Y = \sqrt{\frac{(\mu f^2 + \mu_1(f^2 - g^2))^2 + (2gfr(\mu + \mu_1))^2}{((1-g^2)(f^2-g^2) - \mu g^2 f^2)^2 + (2gfr(g^2 - 1 + \mu g^2))^2}} \tag{13}$$

Note that the case where $\mu_1 = 1$ corresponds to the case where the host system is a mass-spring SDOF system. In this case, Eq. 13 reduces to Eq. 14 which is the same as the one obtained by Tsai and Lin [15] for the case of an undamped SDOF system subjected to a steady-state harmonic base-acceleration and corresponds to case number 5 in [13].

$$Y = \sqrt{\frac{(f^2(\mu + 1) - g^2)^2 + (2gfr(\mu + 1))^2}{((1-g^2)(f^2-g^2) - \mu g^2 f^2)^2 + (2gfr(g^2 - 1 + \mu g^2))^2}} \tag{14}$$

2.3 Orders of magnitude

Before digging into the derivation of optimal TMD parameters, it is important to give orders of magnitude of realistic values for the design parameters in the dimensionless transfer function (Eq. 13). While there are no practical limitations on the values of the stiffness k_d and the damping c_d, it is generally admitted that the mass m_d must remain within a few percent (typically 1 to 3 %) of the mass of the main structure.

One has to be careful not to confuse this actual physical mass ratio with the value of $\mu = m_d/m_{eq}$ in (Eq. 13), which considers m_{eq}, which depends on the location of the TMD and the shape of the mode considered, and is always lower than the actual total mass of the structure. Hence values higher than a few percent can be encountered, but we consider that $\mu = 0.1$ is a maximum value for practical applications.

A look at Eq. 7 shows that $\tilde{m}_{eq}$ is inversely proportional to ψ_{ik}, while m_{eq} (Eq. 6) is inversely proportional to ψ_{ik}^2. μ_1 is therefore proportional to ψ_{ik}, which means that it will have a low value close to the nodes of the mode shapes, and a high value near the maxima of ψ_{ik}.

In much the same way, it can be shown that the mass ratio μ is proportional to ψ_{ik}^2, highlighting the fact that the location of the TMD should be chosen so that it is close to the maxima of ψ_{ik} and as far away as possible from the nodes of the mode shape, in order for the TMD to have efficiency in damping the targeted mode (if μ is small and close to zero, the efficiency of the device is very poor).

It is clear from this discussion that small values of μ_1 are not of practical significance as they would occur due to the very poor choice of the location of the TMD. At this stage, it is difficult however to give practical values of this parameter without considering a specific example, as will be done in Section 4.

3 Equal-peak approach for single-mode approximation and base excitation

The tuning of the TMD parameters aims at minimizing the maximum of Y defined in Eq. 13. A simple yet effective approach is to use the so-called equal peaks method initially presented by Den Hartog [4]. Although this approach has been developed for different configurations (different types of excitations and different quantities of interest [13]), it has never been applied to the non-dimensional transfer function given by Eq. 13.

As stated in the introduction, the equal peak approach does not strictly lead to the optimum set of parameters but has been found to lead to solutions very close to it, with much simpler analytical formulae. It is a two-step procedure that consists first in finding the stiffness of the TMD, which leads to so-called fixed points being at equal height, and second, in finding the best value of damping, which makes these two fixed points very close to the extrema of the transfer function.

Our goal is therefore here to apply this simplified method in order to minimize, in the frequency domain, the maximum of the relative displacement response due to base excitation when a structure is reduced to an SDOF system using the single mode approximation. This will allow to determine the optimal parameters of a mass-spring tuned mass damper as a function of two parameters μ and μ_1 instead of just μ. Although the introduction of this new parameter leads to increased complexity, we will show that in practical applications, it is important to follow this approach for base-excitated systems in order to get an accurate tuning of the TMD.

3.1 Determination of the optimal frequency ratio

The non-dimensional transfer function of Eq. 13 is of the form:

$$Y = \sqrt{\frac{Ar^2 + B}{Cr^2 + D}} \tag{15}$$

Note that C should not be confused with the damping matric $[C]$. The equal peaks method is based on the existence of invariant points in this transfer function, i.e. points where the response does not change when the damping varies. As the damping in this transfer function is represented by the variable r, we can find these invariant points by taking two specific values of $r = \infty$ and $r = 0$ which leads to the equality $A/C = B/D$. For this specific transfer function, A,B, C, and D can all be expressed in the form of $A = a^2$, $B = b^2$, $C = c^2$, and $D = d^2$ so that there are two possible solutions $a/c = b/d$ and $a/c = -b/d$. Replacing by the exact terms from the transfer function, one finds

$$\frac{\mu + \mu_1}{(1+\mu)g^2 - 1} = \pm \frac{(g^2 - f^2)\mu_1 - \mu f^2}{\mu f^2 g^2 - (g^2 - 1)(g^2 - f^2)} \tag{16}$$

3.1.1 P and Q at equal height

The solution with the + sign leads to:

$$(\mu(\mu_1+1)+2\mu_1)\,g^4-\left(2\mu_1+\mu+2(\mu+1)(\mu+\mu_1)f^2\right)g^2+2(\mu+\mu_1)f^2=0 \tag{17}$$

This biquadratic equation in g has two positive solutions g_1 and g_2, corresponding to the abscissas of the two fixed points, which we will call P and Q. For the ordinates of the points P and Q to be identical (which is the idea behind the equal peaks method), one needs to find f so that $Y(f,g_1)=Y(f,g_2)$, which will be true for all values r.

Thus, taking $r=\infty$ leads to $Y^2=A/C$ and we obtain the condition

$$\frac{\mu+\mu_1}{(1+\mu)g_1^2-1}=\pm\frac{\mu+\mu_1}{(1+\mu)g_2^2-1} \tag{18}$$

In the above condition, only the choice of the negative sign gives meaningful solutions; otherwise, $g_1=g_2$ and the two fixed points are not distinct. This condition can be rewritten as:

$$g_1^2+g_2^2=\frac{2}{1+\mu} \tag{19}$$

which gives the sum of the roots of the biquadratic Eq. 17, also given by the ratio of the terms in g^2 and g^4 in this equation, multiplied by (-1). We have

$$\frac{2}{1+\mu}=\frac{2\mu_1+\mu+2(\mu+1)(\mu+\mu_1)f^2}{\mu(\mu_1+1)+2\mu_1} \tag{20}$$

This leads to the direct solution for the frequency ratio $f=f_{opt}$, which results in P and Q being at the same height.

$$f=f_{opt}=\frac{1}{1+\mu}\sqrt{\frac{\mu-\mu^2+2\mu_1}{2(\mu+\mu_1)}} \tag{21}$$

Note that when the main structure is an SDOF system, $\mu_1=1$, and Eq. 21 gives $f=\frac{1}{1+\mu}\sqrt{1-\mu/2}$, which corresponds to the case of the SDOF system subjected to harmonic base-acceleration when relative displacement response is minimized [13]. The new expression derived here is therefore a generalization to the case when $\mu_1\neq 1$, which occurs when the host-structure is an MDOF system reduced to an SDOF using the single mode approximation approach.

We can now derive the exact expression of the roots g_1 and g_2 and compute the value of Y at these two points. Starting again from Eq. 17 in which we replace f^2 by the optimum found for P and Q at equal height (Eq. 21), we have

$$(\mu(\mu_1+1)+2\mu_1)\,g^4-2\frac{\mu(\mu_1+1)+2\mu_1}{\mu+1}g^2+\frac{\mu-\mu^2+2\mu_1}{(\mu+1)^2}=0. \tag{22}$$

The discriminant of this quadratic equation in g^2 is given by

$$\Delta=\frac{4\mu(\mu+\mu_1)(\mu+2\mu_1+\mu_1\mu)}{(1+\mu)^2} \tag{23}$$

so that the values of $g_1^2=g_+^2$ and $g_2^2=g_-^2$ are given by

$$g_\pm^2=\frac{1}{1+\mu}\left(1\pm\sqrt{\frac{\mu(\mu+\mu_1)}{\mu+2\mu_1+\mu_1\mu}}\right) \tag{24}$$

Substituting these values in Eq. 15, taking $r=\infty$ for simplicity (which leads to $Y=\sqrt{A/C}$), we get the value of the equal ordinates Y_{pq} of the points P and Q.

$$Y_{pq}=\pm\frac{1}{\mu}\sqrt{\mu(\mu+\mu_1)(\mu+2\mu_1+\mu_1\mu)}. \tag{25}$$

Let $K=\mu(\mu+\mu_1)(\mu+2\mu_1+\mu_1\mu)$, we have

$$g_\pm^2 = \frac{1}{1+\mu}\left(1\pm\frac{\sqrt{K}}{\mu+2\mu_1+\mu_1\mu}\right), \tag{26}$$

$$Y_{pq} = \pm\frac{1}{\mu}\sqrt{K}. \tag{27}$$

3.1.2 P and R at equal height

The negative sign in Eq. 16 leads to :

$$\mu g^2[(\mu_1 - 1)g^2 + 1] = 0 \tag{28}$$

which gives only one non-trivial positive solution

$$g_3 = 1/(\sqrt{1-\mu_1}) \tag{29}$$

Note that this solution will lead to a real finite value of g_3 only when $\mu_1 < 1$, and that when $\mu_1 = 1$, g_3=0 so that there are only two fixed points. We will call this third point R in the following.

The analysis presented above shows the potential existence of 3 fixed points when $\mu_1 < 1$, while in previous applications of the fixed point method, only two points existed. This raises the question as to which two points should be considered to optimize the TMD.

We already discussed the condition of having P and Q at the same height. If we wish to set P and R at the same height, we have the condition

$$\frac{\mu + \mu_1}{(1+\mu)g_1^2 - 1} = \pm\frac{\mu + \mu_1}{(1+\mu)g_3^2 - 1} \tag{30}$$

where, as before, only the negative sign gives a meaningful solution ($g_1 \neq g_3$). Substituting this time the explicit solution for $g_3 = 1/(\sqrt{1-\mu_1})$ in Eq. 30 gives:

$$g_1^2 = \frac{1 - \mu - 2\mu_1}{(1+\mu)(1-\mu_1)} \tag{31}$$

Since g_1 is also a root of Eq. 17, substituting g_1 from Eq. 31 into Eq. 17 and solving for f leads to the optimum frequency ratio (f_{opt}) for which the two ordinates will be equal:

$$f = f_{opt} = \frac{1}{1+\mu}\sqrt{\frac{1-\mu-2\mu_1}{1-\mu_1}} \tag{32}$$

It is important to recall that this value of f_{opt} exists only for the case when $\mu_1 < 1$ (existence of point R), but the equation also shows that in addition, we need to have $1 - \mu - 2\mu_1 > 0$ which is equivalent to $\mu_1 > (1-\mu)/2$. We know that when P and R are at equal height, g_1 is given by Eq. 31 and $g_3 = 1/(\sqrt{1-\mu_1})$. Taking again $r = \infty$ for simplicity, we obtain the value of Y at points P and R:

$$Y_{pr} = \sqrt{1-\mu_1} \tag{33}$$

3.2 Determination of optimal damping

3.2.1 Optimal damping ratio for P and Q at equal height

The next step in the equal-peak method is to find the optimal damping that leads to the transfer function being maximum at the two points (either P and Q, or P and R) considered. As it is not possible to enforce this condition exactly at these two points, an approximation will be made as in the initial method developed by Den Hartog. Eq. 21 can be used to determine the frequency ratio, which ensures that points P and Q are at equal height. The next step for the equal peaks methods is to determine the optimal damping. Although the idea is to minimize the maximum ($H\infty$-norm) of the transfer function Y, such a closed-form solution is tedious to derive (as it involves a minimization with respect to both f and r) and generally leads to very long expressions.

The approximation in the equal peak method originally proposed by Den Hartog is to first set the frequency ratio f to have the invariant points P and Q at equal heights, and then in a second step, to find the damping values r for which Y is maximum at points P and Q. As these two values are slightly different but close, the average value (computed as the square root of the mean of the square values) is used to get the best compromise. The transfer function is thus not strictly maximum at neither P nor Q, but is very close to the true H_∞ minimum.

We seek to determine r as a function of μ and μ_1 so that the tangent to the graph of Y as a function of g is either horizontal at point P or at point Q. The corresponding calculation can be simplified by the observations below.

1. The derivative $\frac{dY}{dg}$ will vanish if and only if the derivative of Y^2 with respect to g also vanishes. Therefore, one can ignore the large square root in the expression of Y.
2. The expression of Y only involves g through g^2. On the other hand, $\frac{dY}{dg} = 2g\frac{dY}{d(g^2)}$ so that the derivatives vanish simultaneously since we are working with $g > 0$. We can therefore work with the variable g^2 instead of g. To simplify the notations, we will designate the derivative with respect to g^2 with a prime.
3. The derivative of Y (written in the general form of Eq. 15) with respect to g^2 will vanish if and only if $(A'r^2 + B')(Cr^2+D)-(C'r^2+D')(Ar^2+B) = 0$. At points P and Q, this amounts to asking that $(A'r^2+B')-(C'r^2+D')Y_{pq}^2 = 0$. We therefore obtain the value sought for r in the form:

$$r^2 = \frac{Y_{pq}^2 D' - B'}{A' - Y_{pq}^2 C'} \tag{34}$$

The expressions of A, B, C, D and therefore their derivatives A', B', C', D' with f^2 given by Eq. 21 and $g_\pm^2$ given by Eq. 26 as a function of μ and μ_1, as well as the expression Eq. 27 of Y_{pq}^2 as a function of μ and μ_1, are all of the form: $F(\mu,\mu_1) + G(\mu,\mu_1)\sqrt{K}$, where F and G are rational functions (quotients of polynomials). As the value sought for r^2 is obtained by combining these expressions with the 4 operations (addition, substraction, multiplication and division), we deduce below that the expression for r^2 is itself of this form. It is obvious that the sum and the difference of such expressions have the same form. For the product, we have

$$(F_1 + G_1\sqrt{K})(F_2 + G_2\sqrt{K}) = (F_1F_2 + G_1G_2K) + (F_2G_1 + F_1G_2)\sqrt{K} \tag{35}$$

For the quotient, we have (via multiplication and division by the conjugated binomial)

$$\frac{F_1 + G_1\sqrt{K}}{F_2 + G_2\sqrt{K}} = \frac{(F_1F_2 - G_1G_2K)}{F_2^2 - G_2^2K} + \frac{(F_2G_1 - F_1G_2)}{F_2^2 - G_2^2K}\sqrt{K} \tag{36}$$

The objective is therefore to reduce to an expression of the form $F + G\sqrt{K}$ at each stage of the calculation to avoid having to handle overly complicated expressions. Noting that the values of g^2 in P and in Q differ only by the sign in front of $\sqrt{K}$, we can perform both calculations at the same time and will show that the expression of r^2 for P and Q also only differ by the sign in front of $\sqrt{K}$, hence if $r_{P,Q}^2 = F \pm G\sqrt{K}$, the average value $r^2 = \frac{1}{2}\left(r_P^2 + r_Q^2\right)$ is equal to F. The detailed calculation is given in Section 6.1 (Annex A) and leads to the following expression for the optimal damping:

$$r^2 = r_{opt}^2 = \frac{\mu(\mu_1\mu^2 + 6\mu_1^2 + 13\mu_1\mu + 5\mu^2 - \mu)}{8(\mu - \mu^2 + 2\mu_1)(\mu + \mu_1)(\mu + 1)} \tag{37}$$

It is worth noting that when $\mu_1 = 1$, the expression for r_{opt} reduces to the one given by Warburton [13]:

$$r_{opt}^2 = \frac{3\mu}{8(1+\mu)(1-\mu/2)} \tag{38}$$

3.2.2 Optimal damping ratio for P and R at equal height

As in the case for P and Q, we seek to determine r as a function of μ and μ_1 so that the tangent to the graph of Y as a function of g is either horizontal at point P or at point R. The same observations as for the case with P and Q apply; therefore, the procedure consists in computing the value of r^2 using Eq. 34. In this case, however, the two roots g_1 and g_3 cannot be expressed in a compact, uniform manner with a $\pm$ sign to differentiate them, so a separate calculation is needed for each point. The calculations are given in Section 6.2 (Annex B) and lead to the following optimal values for r^2:

$$r_P^2 = \frac{\mu(1-\mu_1)}{2(\mu+1)(1-\mu-2\mu_1)}. \tag{39}$$

$$r_R^2 = -\frac{1}{2(\mu+1)^2(1-\mu-2\mu_1)}(5\mu\mu_1 + \mu^2\mu_1 - \mu + \mu^2 + 2\mu_1^2)(\mu+\mu_1). \tag{40}$$

The optimal damping is given by $r_{opt}^2 = \frac{1}{2}(r_R^2 + r_P^2)$. We obtain

$$r^2 = r_{opt}^2 = \frac{1}{2}(r_R^2 + r_P^2) = \frac{\mu - 3\mu\mu_1 - \mu^2\mu_1 - \mu_1^2}{2(1+\mu)^2(1-\mu-2\mu_1)} \tag{41}$$

3.3 Choice of the invariant points for the TMD optimization

We aim at finding the intervals of the parameters μ and μ_1 in which we need to use either the formula for P and Q (Eqs. 21 and 37) at the same height or the formula for P and R (Eqs. 32 and 41). Fig. 2 shows the evolution of the roots (frequencies) corresponding to the invariant points at equal height, for a value of $\mu = 0.1$ and values of μ_1 between -1 and +1. The grey curves show the two roots of Eq. 17 when f is given by Eq. 21 (P and Q at the same height). As μ_1 increases, points P and Q tend to get closer together until $\mu_1 = -\mu$ (-0.1 in the present case), where the two points merge. Looking at the expression of the roots (Eq. 26), we see that this happens when

$$\sqrt{K} = \sqrt{\mu(\mu + \mu_1)(\mu + 2\mu_1 + \mu_1\mu)} = 0 \tag{42}$$

hence when $\mu_1 = -\mu$. The expression of the roots also shows that they tend to ∞ when $\mu + 2\mu_1 + \mu_1\mu = 0$, hence the roots reappear at $\pm\infty$ when $\mu_1 > \frac{-\mu}{2+\mu}$. Note that this is also the point after which f^2 is positive again.

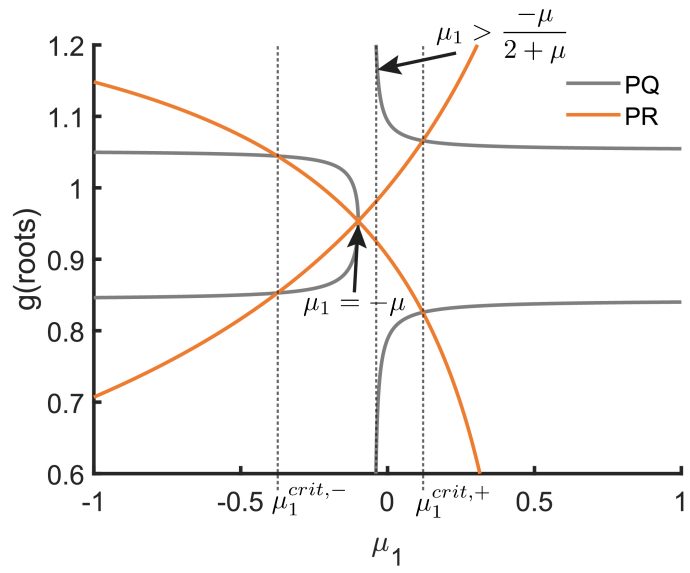

Fig. 2: Evolution of the roots corresponding to equal height of invariant points as a function of μ_1 ($\mu = 0.1$), for the cases when P and Q, or P and R are set at equal height.

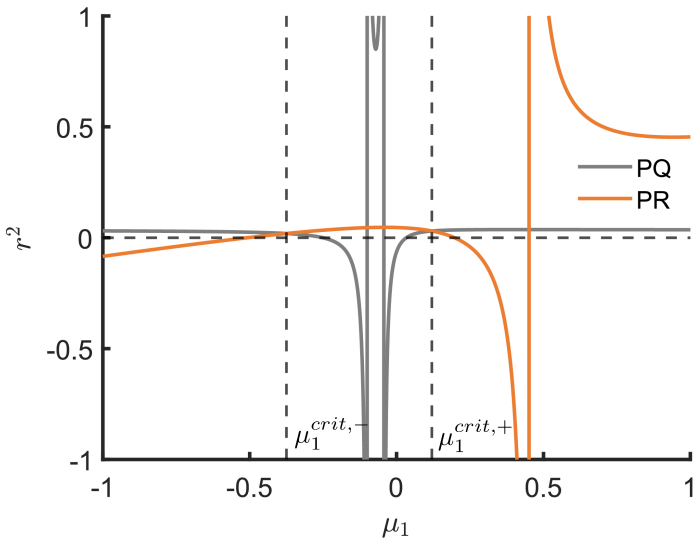

Fig. 3: Evolution of r^2 as a function of μ_1 ($\mu = 0.1$), using (Eq. 37) (PQ) and (Eq. 41) (PR)

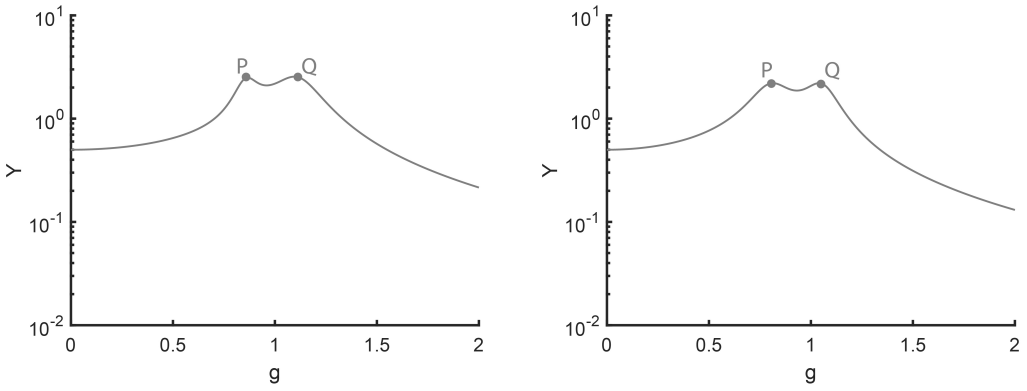

Fig. 4: Transfer function Y when the TMD is optimally tuned - $\mu = 0.1$, $\mu_1^{crit,-} = -0.375$, $\mu_1^{crit,+} = 0.12$ (left:$\mu_1 = -0.6$, right:$\mu_1 = 0.4$)

The orange curves show the evolution of the two roots corresponding to equal height when f is given by Eq. 32 (P and R at equal height). Note that by using Eq. 21, point P changes. Starting from $\mu_1 = -1$, we notice that the roots are more separated than in the case when P and Q are set at equal height, until they merge with the grey curves. This is the point where the roots taken either from Eq. 21 or Eq. 32 are the same, which means that f has the same value, thus

$$\frac{1}{\mu+1}\sqrt{\frac{1-\mu-2\mu_1}{1-\mu_1}} = \frac{1}{\mu+1}\sqrt{\frac{\mu-\mu^2+2\mu_1}{2(\mu+\mu_1)}} \tag{43}$$

which can be simplified to

$$\mu_1^2 + \frac{5\mu+\mu^2}{2}\mu_1 - \frac{\mu-\mu^2}{2} = 0 \tag{44}$$

The roots of this equation are given by

$$\mu_1^{crit,\pm} = \frac{-5\mu-\mu^2 \pm \sqrt{8\mu+17\mu^2+10\mu^3+\mu^4}}{4} \tag{45}$$

and are marked with two vertical dashed lines on the plot (when $\mu = 0.1$ as in the figure, we have $\mu_1^{crit,-} = -0.375$ and $\mu_1^{crit,+} = 0.12$). Again, we see that after the second root (second vertical line), the solutions given by the orange curves are more distant than the grey curves. The solutions for P and R cease to exist when $(1-\mu-2\mu_1) < 0$ and $(1-\mu_1) > 0$ that is, in our plot, between $\mu_1 = 0.45$ and μ_1=1.

Fig. 3 shows the evolution of r_{opt}^2 as a function of μ_1 for the same fixed value of $\mu = 0.1$, using the formula for optimal damping when choosing P and Q at the same height (Eq. 37) or P and R at the same height (Eq. 41). The figure shows that for some values of μ_1, r^2 is negative, so that there is no possibility to optimally tune the damping. For values of $\mu_1 < \mu_1^{crit,-}$ and $\mu_1 > \mu_1^{crit,+}$, the value of r^2 computed according to Eq. 37 is always positive. When tuning to have P and R at the same height for values of μ_1 between $\mu_1^{crit,-}$ and $\mu_1^{crit,+}$, the values of r^2 computed according to Eq. 41 are also always positive. Note that there is a small region around each critical values of μ_1 where both equations could be used for the tuning, as f exists and r^2 is positive.

In Fig. 4, we represent the transfer function of the host system Y when optimal tuning is done according to the P and Q rules for values of μ_1 used in outside of the range $[\mu_1^{crit,-}, \mu_1^{crit,+}]$ ($\mu_1 = -0.6$ and $\mu_1 = 0.4$). In both cases, we see that the use of tuning rules for P and Q lead to equal peaks.

As stated above, there are small intervals close to $\mu_1^{crit,-}$ and $\mu_1^{crit,+}$ where the value of r^2 is positive for both cases so that tuning is possible according to the two equations. Different examples are shown in Figs. 5 and 6. The figures show that choosing P and R at the same height when μ_1 is between $\mu_1^{crit,-}$ and $\mu_1^{crit,+}$ is a better choice as the maximum of $Y(g)$ is lower, and that choosing P and Q when μ_1 is outside of this interval leads also to a lower maximum for $Y(g)$. It can also be seen in these figures that when the non-optimal choice is made for the tuning rule, the transfer function does not show strictly equal peaks. We can conclude that the critical values of μ_1 set the limit for the choice of the tuning rules (P and R inside the interval of critical values, and P and Q outside). Following up on our discussion in Section 2.3, where we stated that small values of μ_1 are not of practical interest, we can deduce that the equations for P and Q will generally be used in practice.

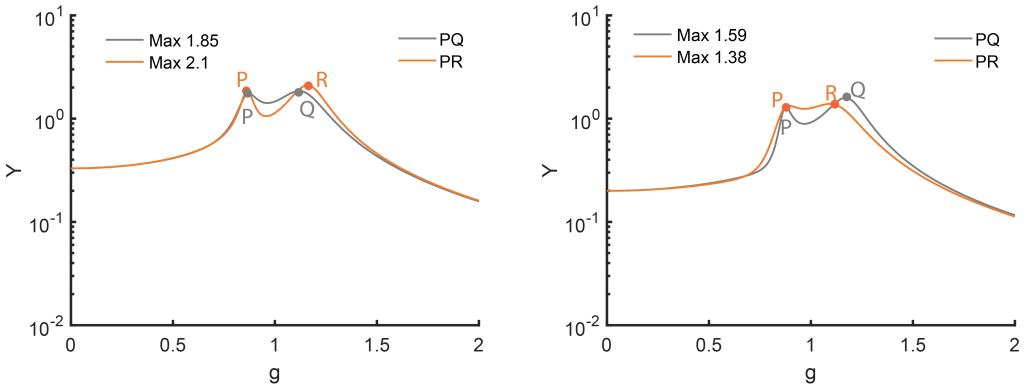

Fig. 5: Comparison of transfer function Y when the TMD is optimally tuned with P and Q or P and R at equal height - $\mu = 0.1$, $\mu_1^{crit,-} = -0.375$, $\mu_1^{crit,+} = 0.12$ (left:$\mu_1 = -0.43$, right:$\mu_1 = -0.3$, values close to $\mu_1^{crit,-}$)

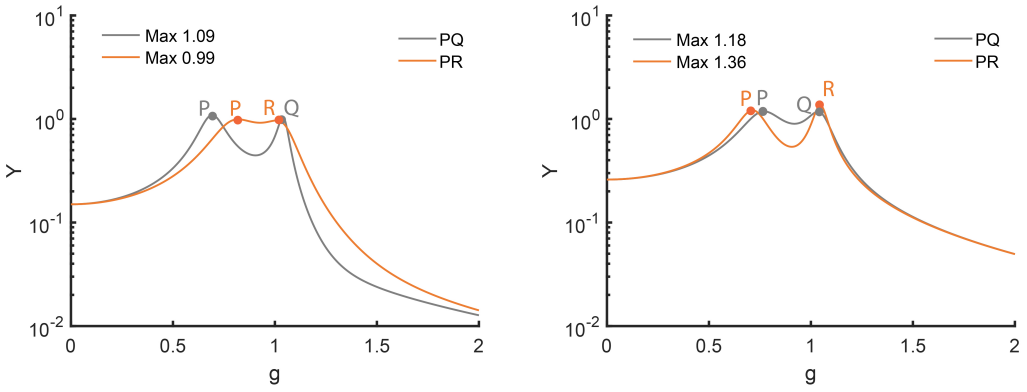

Fig. 6: Comparison of transfer function Y when the TMD is optimally tuned with P and Q or P and R at equal height - $\mu = 0.1$, $\mu_1^{crit,-} = -0.375$, $\mu_1^{crit,+} = 0.12$ (left:$\mu_1 = 0.05$, right:$\mu_1 = 0.16, \mu = 0.1$, values close to $\mu_1^{crit,+}$)

Although, as discussed before, of little practical use, we represent in Figs. 7 and 8 cases where μ_1 lies between the critical values and only the tuning rules for P and R can be used. The curves confirm that the tuning rules allow to reach equal peaks. Note that for $\mu_1 = -0.101$ the roots coallesce and we have a single highly damped peak.

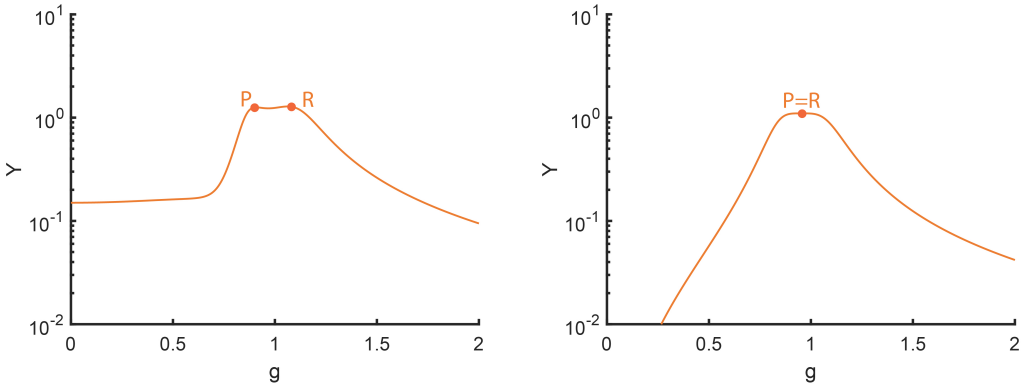

Fig. 7: Transfer function Y when the TMD is optimally tuned - $\mu = 0.1$, $\mu_1^{crit,-} = -0.375$, $\mu_1^{crit,+} = 0.12$ (left:$\mu_1 = -0.25$, right:$\mu_1 = -0.101$)

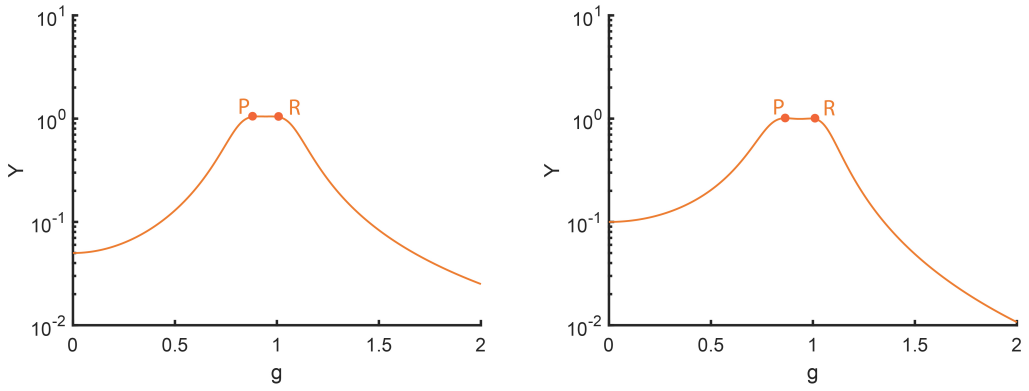

Fig. 8: Transfer function Y when the TMD is optimally tuned - $\mu = 0.1$, $\mu_1^{crit,-} = -0.375$, $\mu_1^{crit,+} = 0.12$ (left:$\mu_1 = -0.04$, right:$\mu_1 = 0$)

4 Practical example: high-rise building

As TMDs are mostly installed on tall buildings, we consider the simplified model of a high-rise building with a large concrete core of height $L = 140$ m (Fig. 9(a)). The concrete's mechanical properties are given by its Young's modulus $E = 30$ GPa, Poisson's ratio $\nu = 0.2$, and density $\rho = 2200$ kg/m^3, already used in [16]. The building is modelled as a vertical cantilever beam with a hollow box-type cross-section of external cross-section of 20 m $\times$ 20 m and a thickness of 30 cm. The modal damping ratios of the building are assumed to be very small. The cross-sectional

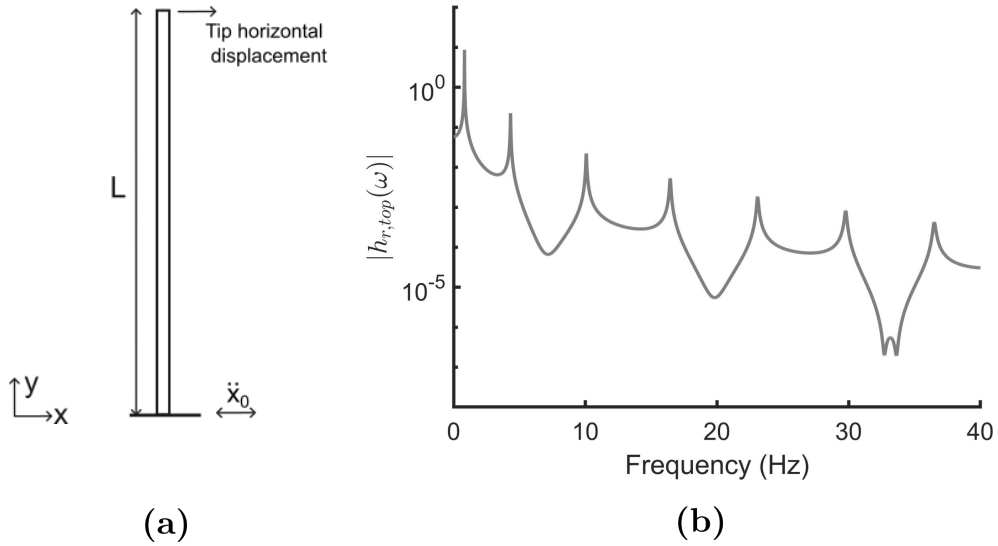

Fig. 9: (a) High-rise building modeled as a cantilever beam excited horizontally at its base (left figure), and (b) frequency response function of the relative displacement of top floor of the example building model (right figure)

area of the beam is $A_{cross} = 20^2 - (20 - 2 \times 0.3)^2 = 23.64$ m^2, and the total mass is $M_{tot} = A_{cross} \times \rho \times L = 7.28 \times 10^6$ kg. The finite element model of the beam is constructed in the Structural Dynamics Toolbox under Matlab [17] using Euler-Bernoulli beam elements with shear correction factors for thick beams. The beam model contains 21 nodes; the first node represents the ground to which base acceleration is imposed, and the remaining 20 nodes have two degrees-of-freedom each (one translation and one rotation as the motion is restricted in one plane for this simple example). The model has 40 DOFs in total. The frequency response function of the top floor's (or tip of the cantilever) relative displacement divided by the unitary input acceleration, noted $|h_{r,top}(\omega)|$ is represented in Fig. 9(b). The first 10 natural frequencies are 0.82, 4.32, 10.07, 16.45, 23.08, 29.77, 36.50, 43.25, 50.04, and 56.87 Hz. Note that the ratio of the consecutive frequencies for the first three modes is, respectively, 5.3 (Mode-2 to Mode-1), 2.3 (Mode-3 to Mode-2), and 1.6 (Mode-4 to Mode-3). The figure also shows that the first mode is much more excited than the

following ones, and that the general trend is a decrease of the contribution of the modes, as can be expected and already discussed, for base excitation.

As discussed by Warburton in [18], the equivalent SDOF approach (for the fundamental mode) is valid when the ratio of the two consecutive modes is higher than 2-3 depending on the damper mass. The criteria is satisfied in our example, at least for the fundamental mode. For higher modes, the frequency ratio suggests that there may be effects of modal interactions.

In order to demonstrate the practically relevant cases, we need to identify the critical modes by analysing the modal participation and modal amplitudes. The participation of different modes in the overall response for a base excitation is shown in Fig. 10(a), which is assessed using the relative participation factor of i^{th} mode defined as $\frac{|\Gamma_i|}{|\Gamma|_{\max}}$, where $\Gamma_i = \{\psi_i\}^T[M]\{T\}$, $\{\psi_i\}$ is the i^{th} mode-shape vector, $\{T\}$ the influence vector, and $|\Gamma|_{\max}$ = the maximum absolute value of modal participation vector amongst all the modes. As shown in Fig. 10, the maximum contribution comes from the first two modes and reduces drastically after that. Hence, we will focus on the first two modes only. The first two mode shapes are plotted in Fig. 10(b).

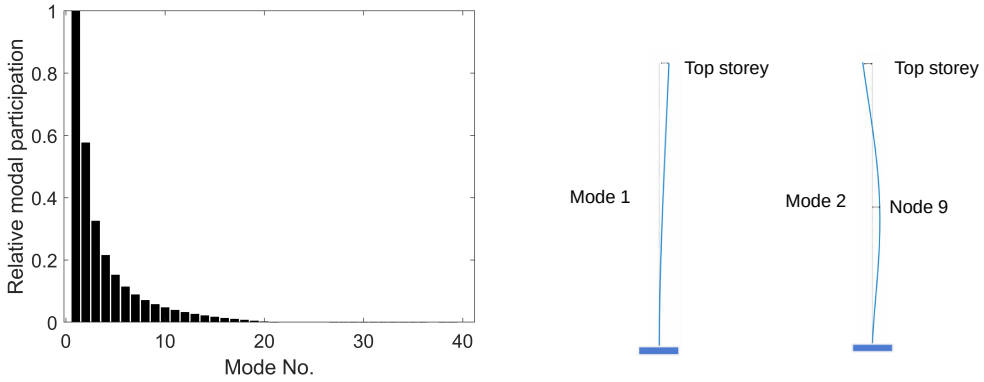

Fig. 10: (a) Relative modal participation factors (left figure) and (b) first two modes of the high-rise building (right figure)

4.1 Equivalent SDOF parameters and location of the TMD

In order to tune the TMD device for the example building model, a practical value of damper mass m_d is assumed to be 1% of the total building mass ($m_d = 0.01 \times M_{tot} = 7.28 \times 10^4$ kg). The mass of the equivalent SDOF system m_{eq} (and, hence, the mass ratio μ and the critical values $\mu_1^{crit,\pm}$) depend on the mode to be tuned and the location of the attachment of the TMD (see Eq. (6)). The second mass ratio μ_1 also depends on the modal amplitudes and, in addition, on the modal participation factor. The variation of μ, $\mu_1^{crit,+}$, $\mu_1^{crit,-}$, and μ_1 with TMD location is shown in Fig. 11 for the first two modes. Based on this analysis, some interesting observations can be made:

1. The equivalent mass ratio μ changes with the TMD location. The choice of the maximum mass of the TMD should however be made based on practical considerations of maximum acceptable added mass. It is clear that after this mass has been chosen, the TMD should be located at the maximum of the mode shapes in order to have a higher equivalent mass ratio μ, hence a better efficiency of the device.
2. The second mass ratio μ_1 follows the same trend as the mode shape and is maximum where the mode shapes are maximum (as μ). As discussed above, this is where the TMD should be placed to have good efficiency; therefore, only these values of μ_1 are of practical interest. In particular, the figures show that
   - in the case of Mode 1, $\mu_1 > \mu_1^{crit,+}$ and therefore Eqs. (21) and (37) will be used to tune the TMD.
   - In the case of Mode 2, there are two possible locations for optimal placement of the TMD. One is at node 9 (first maximum of the mode shape), and the other one is at node 20 (second maximum). In both cases, the values of μ_1 do not lie in the critical range.

   The observations above show that only the formulae for μ_1 outside of the critical range (Eqs. (21) and (37)) are of practical use, as already discussed in Section 3.3.

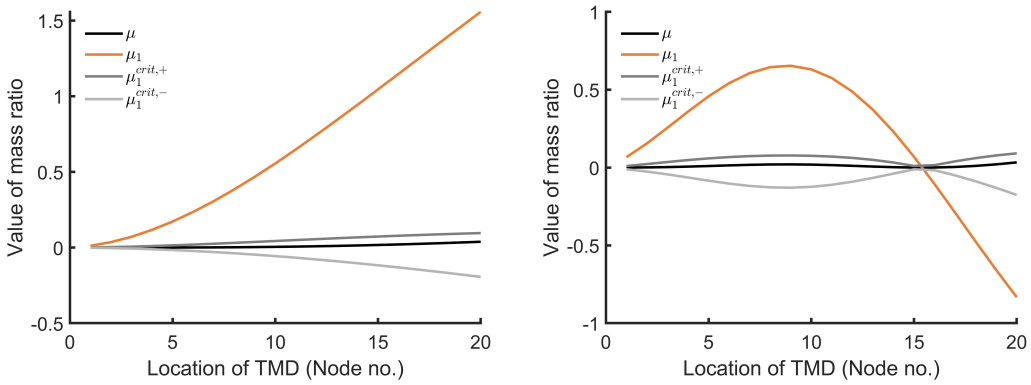

Fig. 11: Variation of the two mass ratios (μ and μ_1) and the critical limits ($\mu_1^{crit,+}$, $\mu_1^{crit,-}$) with the location of attachment of TMD when target mode is: (a) first mode (left figure) and (b) second mode of example building (right figure)

4.2 Illustration for different modes and TMD locations

Three example cases are considered where the TMD is placed at th top of the building (node 20) to damp modes 1 or 2, or at node 9 to damp mode 2 (first maximum of second mode shape). For each case, optimal tuning and damping ratios are computed using the new approach developed in this paper in Section 3 (New) and compared with the result using Warburton's formulae (WB) which only takes into account one mass ratio μ:

$$f = \frac{1}{1+\mu}\sqrt{1-\mu/2} \qquad r_{opt}^2 = \frac{3\mu}{8(1+\mu)(1-\mu/2)} \tag{46}$$

The optimum parameters are also evaluated using numerical optimization in MATLAB, where the objective function to minimize is the maximum of the transfer function computed with the two DOFs model using the equivalent parameters for the host system.

The results for the three cases are given in Table 1 where the optimum damping and stiffness parameters of the TMD are given using the three optimization methods. The results show that the new approach gives optimum parameters very close to the true optimum obtained with numerical optimization, while the parameters obtained with Warburton's formulae are slightly different.

Table 1: Optimal parameters for the three cases using Warburton(WB) formulae, the new proposed formulae (New) and numerical optimization (Num)

Mode	DOF	μ_1	μ	b_{wb} N/(m/s)	k_{wb} N/m	b_{new} N/(m/s)	k_{new} N/m	b_{num} N/(m/s)	k_{num} N/m
1	39	1.5574	0.0386	$8.511\,10^4$	$1.750\,10^6$	$8.517\,10^4$	$1.762\,10^6$	$8.489\,10^4$	$1.762\,10^6$
2	39	-0.8327	0.0333	$41.99\,10^4$	$49.31\,10^6$	$41.64\,10^4$	$51.23\,10^6$	$41.82\,10^4$	$51.23\,10^6$
2	17	0.6538	0.0205	$33.59\,10^4$	$50.89\,10^6$	$33.54\,10^4$	$50.62\,10^6$	$33.48\,10^4$	$50.62\,10^6$

The frequency response functions $Y(g)$ obtained with these three sets of optimum parameters are compared in Fig. 12 for the three different configurations considered. It is clear that for all cases, the new formulae lead to an equal-peak design, and the transfer function matches exactly with the numerical optimum, on the contrary to the WB approach. Note that as highlighted in Section 2.3, the effective mass ratio ranges from 2 to 4 % depending on the location of the TMD and mode to be damped, while the physical mass ratio was set to 1%.

It is important to note that this result is obtained with the reduced two DOFs system where the building is represented only by the contribution of the targeted mode. As already discussed before, while this is usually a very good approximation for the first mode, the modal interactions can become more important with increasing mode number. It is especially the case for base excitation, as evidenced by the modal participation factors represented in Fig. 10(a). In Fig. 13, we compare the transfer function obtained with the full model, using the parameters obtained with the new

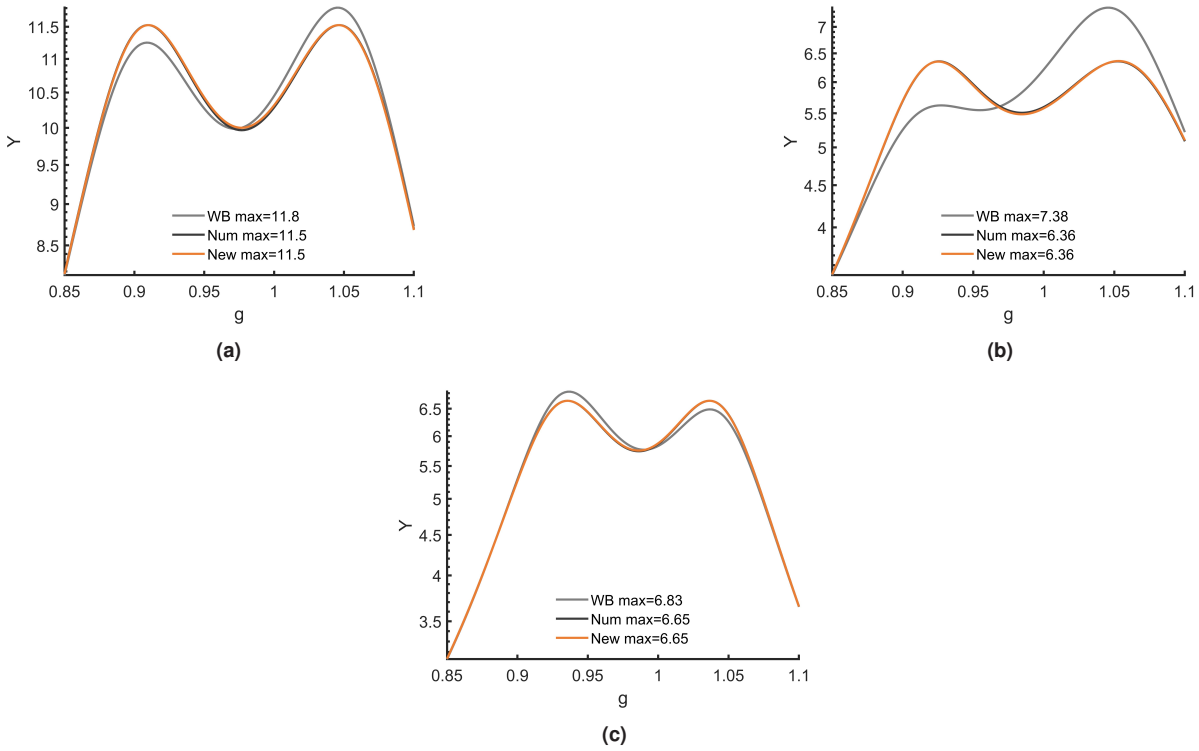

Fig. 12: Comparison of FRFs of relative displacement at the location and in the direction of the TMD, considering the equivalent SDOF host-system for : (a) Case-1 (Mode 1, node 20, $\mu = 0.039, \mu_1 = 1.58$), (b) Case-2 (Mode 2, node 20, $\mu = 0.033, \mu_1 = -0.83$)), and (c) Case-3 (Mode 2, node 9, $\mu = 0.02, \mu_1 = 0.65$))

approach (New), to the case where numerical optimization is performed using the full model (resulting in equal peaks).

It is clear from the figures that we preserve almost equal-peaks only in the case of the first mode, where modal interactions are not important. For the second mode, the influence of the first mode is important and results in an imbalance of the peaks. This is more pronounced when the TMD is attached to the tip of the beam as this is where the contribution of mode 1 is the highest (Fig. 13(b)).

The influence of modal interactions for the tuning of TMDs was already raised by Krenk and Høgsberg in [19], however, we found that the solution proposed in their paper does not address the problem adequately for equal-peak approaches. Further research is needed to address the problem related to modal interactions, which lies outside of the scope of this paper.

5 Conclusions

The work presented in this paper deals with the optimal tuning of tuned mass dampers (TMDs) for complex base-excited systems. It starts with the observation that there is no satisfactory analytical approach in the literature to deal with this problem. This is essentially because the traditional single mode approximation is not valid for base-excited systems.

We therefore propose an improved version of the single mode approximation, which leads to the appearance of a second mass ratio in the transfer function of the host-system. With this modified transfer function, we find analytical formulae for the optimal stiffness and damping coefficients of the TMD using the equal peak method. The resulting formulae are a function of the typical mass ratio μ and of a second mass ratio μ_1, and reduce to the well-known formulae of Warburton when $\mu_1 = 1$, which shows their consistency. In the derivation of the analytical formulae, we show that for certain values of the set of parameters (μ, μ_1) there are three and not two invariant points, and a

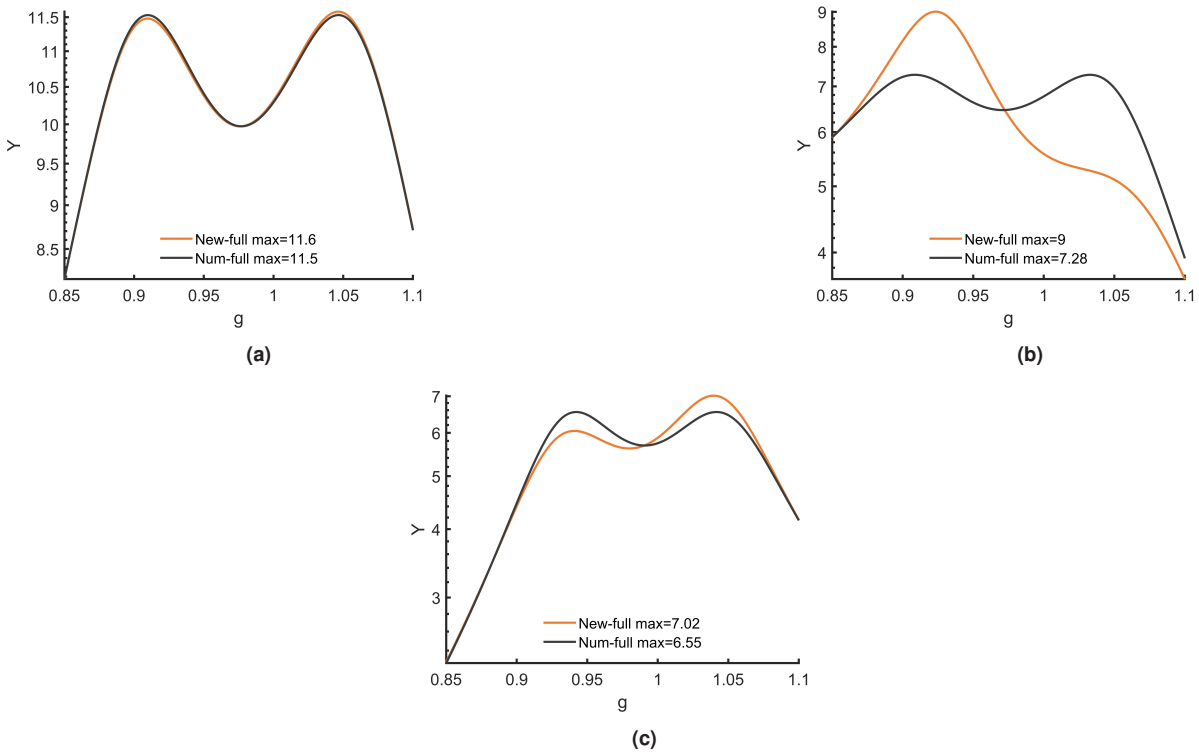

Fig. 13: Comparison of FRFs of relative displacement at the location and in the direction of the TMD using the full and the reduced model : (a) Case-1 (Mode 1, node 20), (b) Case-2 (Mode 2, node 20), and (c) Case-3 (Mode 2, node 9)

discussion on the adequate choice of the two invariant points to be set at equal height leads to the derivation of two sets of equations, depending on the set of values of (μ, μ_1). A further discussion shows that in practice, due to the choice of the optimal location of the TMD in order to have a sufficient effect on the host-structure, only the first set of tuning rules is to be used in practical cases.

The use of the analytical formulae for the tuning of a TMD attached to a MDOF model of a high-rise building excited through its base is then illustrated. The results show that, on the contrary to the approach of Warburton (corresponding to $\mu_1 = 1$, which is not adequate when single-mode approximation is used for a base-excited system), the new approach developed in this paper leads to equal peaks when using the reduced two DOFs system of the host-system with the TMD attached. When using the full model of the structure and the optimal parameters derived analytically based on the improved single mode approximation, the results are good when tuning the TMD to the first mode of the building, but the peaks are unbalanced for the second mode, in particular when the TMD is placed at a position where the response of the first mode is important. This is due to modal interactions, which are not taken into account in the analytical formulae. The tuning of the TMD for base-excitation taking into account modal interactions would result in the modification of the transfer function being minimized and hence requires additional lengthy calculations, which are out of the scope of this paper but are seen as a possible continuation and further improvement of this work.

Authors' Contributions

Shashank Pathak, conceptualized and analysed the problem and prepared the first draft of the paper. Frédéric Bourgeois, carried out the detailed mathematical derivations of different formulae mentioned in the paper for the calculation of f_{opt} and r_{opt}. Arnaud Deraemaeker, proposed the main idea of this paper and then carried out detailed discussions with Shashank Pathak to solve the problem. He also worked on the final version of the paper. All authors reviewed the final manuscript.

References

[1] S. Elias and V. Matsagar. Research developments in vibration control of structures using passive tuned mass dampers. *Annual Reviews in Control*, 44:129–156, 2017. doi:https://doi.org/10.1016/j.arcontrol.2017.09.015.

[2] F. Yang, R. Sedaghati, and E. Esmailzadeh. Vibration suppression of structures using tuned mass damper technology: A state-of-the-art review. *Journal of Vibration and Control*, 28(7-8):812–836, 2022. doi:https://doi.org/10.1177/1077546320984305.

[3] L. Koutsoloukas, N. Nikitas, and P. Aristidou. Passive, semi-active, active and hybrid mass dampers: A literature review with associated applications on building-like structures. *Developments in the Built Environment*, page 100094, 2022. doi:https://doi.org/10.1016/j.dibe.2022.100094.

[4] J. Den Hartog. *Mechanical vibrations*. McGraw-Hill Book Company, 1956.

[5] R. G. Jacquot and D. L. Hoppe. Optimal random vibration absorbers. *Journal of the Engineering Mechanics Division*, 99(3): 612–616, 1973. doi:https://doi.org/10.1061/JMCEA3.0001771.

[6] D. L. Bartel and A. I. Krauter. Time domain optimization of a vibration absorber. *Journal of Engineering for Industry*, 93(3): 799–803, 1971. doi:https://doi.org/10.1115/1.3428016.

[7] Y. Wang and S. Cheng. The optimal design of dynamic absorber in the time domain and the frequency domain. *Applied Acoustics*, 28(1):67–78, 1989. doi:https://doi.org/10.1016/0003-682X(89)90032-7.

[8] O. Nishihara and T. Asami. Closed-form solutions to the exact optimizations of dynamic vibration absorbers (minimizations of the maximum amplitude magnification factors). *J. Vib. Acoust.*, 124(4):576–582, 2002. doi:https://doi.org/10.1115/1.1500335.

[9] A. Ghosh and B. Basu. A closed-form optimal tuning criterion for tmd in damped structures. *Structural Control and Health Monitoring: The Official Journal of the International Association for Structural Control and Monitoring and of the European Association for the Control of Structures*, 14(4):681–692, 2007. doi:https://doi.org/10.1002/stc.176.

[10] M. Argenziano, D. Faiella, A. Carotenuto, E. Mele, and M. Fraldi. Generalization of the Den Hartog model and rule-of-thumb formulas for optimal tuned mass dampers. *Journal of Sound and Vibration*, 538:117213, 2022. doi:https://doi.org/10.1016/j.jsv.2022.117213.

[11] G. Warburton and E. Ayorinde. Optimum absorber parameters for simple systems. *Earthquake Engineering & Structural Dynamics*, 8(3):197–217, 1980. doi:https://doi.org/10.1002/eqe.4290080302.

[12] R. Jacquot. Optimal dynamic vibration absorbers for general beam systems. *Journal of Sound and Vibration*, 60(4):535–542, 1978. doi:https://doi.org/10.1016/S0022-460X(78)80090-X.

[13] G. Warburton. Optimum absorber parameters for various combinations of response and excitation parameters. *Earthquake Engineering & Structural Dynamics*, 10(3):381–401, 1982. doi:https://doi.org/10.1002/eqe.4290100304.

[14] M. N. Hadi and Y. Arfiadi. Optimum design of absorber for mdof structures. *Journal of Structural Engineering*, 124(11): 1272–1280, 1998. doi:https://doi.org/10.1061/(ASCE)0733-9445(1998)124:11(1272).

[15] H.-C. Tsai and G.-C. Lin. Optimum tuned-mass dampers for minimizing steady-state response of support-excited and damped systems. *Earthquake engineering & structural dynamics*, 22(11):957–973, 1993. doi:https://doi.org/10.1002/eqe.4290221104.

[16] M. Soubeyroux, C. Dumoulin, and A. Deraemaeker. Optimization of tuned mass damper parameters based on numerical optimization and model reduction. *ISMA 2018*, pages 201–251, 2018.

[17] E. Balmès. Structural dynamics toolbox, for use with matlab.

[18] G. Warburton. Optimum absorber parameters for minimizing vibration response. *Earthquake engineering & structural dynamics*, 9(3):251–262, 1981. doi:https://doi.org/10.1002/eqe.4290090306.

[19] S. Krenk and J. Høgsberg. Tuned resonant mass or inerter-based absorbers: unified calibration with quasi-dynamic flexibility and inertia correction. *Proceedings of the Royal Society A: Mathematical, Physical and Engineering Sciences*, 472(2185): 20150718, 2016. doi:https://doi.org/10.1098/rspa.2015.0718.

6 Annex

6.1 Annex A : Calculation of optimal damping r for P and Q at the same height

We differentiate with respect to g^2 the 4 functions appearing in Eq. 15:

$$\begin{aligned} A &= 4f^2g^2(\mu+\mu_1)^2, \\ B &= \left(\mu_1 g^2 - (\mu+\mu_1)f^2\right)^2, \\ C &= 4f^2g^2\left((1+\mu)g^2-1\right)^2, \\ D &= \left(\mu f^2 g^2 - (g^2-1)(g^2-f^2)\right)^2, \end{aligned}$$

to get

$$\begin{aligned} A' &= 4f^2(\mu+\mu_1)^2, \\ B' &= 2\mu_1\left(\mu_1 g^2 - (\mu+\mu_1)f^2\right), \\ C' &= 4f^2((1+\mu)g^2-1)\left((1+\mu)g^2-1+2(1+\mu)g^2\right) \\ &= 4f^2((1+\mu)g^2-1)(3(1+\mu)g^2-1), \\ D' &= 2\left(\mu f^2 g^2-(g^2-1)(g^2-f^2)\right)(\mu f^2-2g^2+f^2+1) \\ &= \frac{2}{\mu+\mu_1}((1+\mu)g^2-1)\left(\mu_1 g^2-(\mu+\mu_1)f^2\right)\left((\mu+1)f^2+1-2g^2\right). \end{aligned}$$

which gives for $Y_{pq}^2 C'$:

$$\begin{aligned} Y_{pq}^2 C' &= 4f^2\frac{(\mu+\mu_1)(\mu+2\mu_1+\mu_1\mu)}{\mu}\left((1+\mu)g^2-1\right)\left(3(1+\mu)g^2-1\right) \\ &= 4f^2\left(3(\mu+\mu_1)^2 \pm 2\frac{(\mu+\mu_1)}{\mu}\sqrt{K}\right). \end{aligned}$$

where we have used the expression of g^2 at point P and Q given by Eq. 26 and Y_{pq} by Eq. 27. This leads to $A' - Y_{pq}^2 C'$:

$$\begin{aligned} A' - Y_{pq}^2 C' &= 4f^2\left((\mu+\mu_1)^2 - 3(\mu+\mu_1)^2 \mp 2\frac{(\mu+\mu_1)}{\mu}\sqrt{K}\right). \\ &= -4\frac{\mu-\mu^2+2\mu_1}{(\mu+1)^2}\left(\mu+\mu_1 \pm \frac{1}{\mu}\sqrt{K}\right). \end{aligned}$$

where we have replaced f^2 using Eq. 21. We then express $1/(A' - Y_{pq}^2 C')$:

$$\begin{aligned} \frac{1}{A' - Y_{pq}^2 C'} &= -\frac{(\mu+1)^2}{4(\mu-\mu^2+2\mu_1)}\left(\mu+\mu_1 \mp \frac{1}{\mu}\sqrt{K}\right) \\ &\quad \times \frac{1}{(\mu+\mu_1)^2 - \frac{(\mu+\mu_1)(\mu+2\mu_1+\mu_1\mu)}{\mu}} \\ &= \frac{\mu(\mu+1)^2}{4(\mu-\mu^2+2\mu_1)^2(\mu+\mu_1)}\left(\mu+\mu_1 \mp \frac{1}{\mu}\sqrt{K}\right). \end{aligned}$$

On the other hand, we calculate the expression $Y_{pq}^2 D'$:

$$\begin{aligned} Y_{pq}^2 D' &= \frac{2(\mu+2\mu_1+\mu_1\mu)}{\mu}\left(\pm\frac{\sqrt{K}}{(\mu+2\mu_1+\mu_1\mu)}\right)\left(\mu_1 g^2-(\mu+\mu_1)f^2\right) \\ &\quad \times\left((\mu+1)f^2+1-2g^2\right) \\ &= \frac{2}{\mu+1}\left(\mu_1 g^2-(\mu+\mu_1)f^2\right)\left(-2(\mu+\mu_1) \pm \frac{\mu+2\mu_1-1}{2(\mu+\mu_1)}\sqrt{K}\right). \end{aligned}$$

We calculate the factor $\mu_1 g^2 - (\mu+\mu_1)f^2$ separately, replacing g^2 and f^2 by their expressions in terms of μ and μ_1 as previously:

$$\begin{aligned} &\mu_1 g^2 - (\mu+\mu_1)f^2 \\ &= \frac{1}{(1+\mu)^2}\left(\frac{\mu(\mu+2\mu_1-1)}{2} \pm \frac{\mu_1(1+\mu)}{\mu+2\mu_1+\mu_1\mu}\sqrt{K}\right). \end{aligned}$$

We finally get the expression of $Y_{pq}^2 D' - B'$

$$\begin{aligned} & Y_{pq}^2 D' - B' \\ = \; & \frac{2}{\mu+1}\left(\mu_1 g^2 - (\mu+\mu_1) f^2\right) \\ & \times\left(-2(\mu+\mu_1) - (\mu+1)\mu_1 \pm \frac{\mu+2\mu_1-1}{2(\mu+\mu_1)}\sqrt{K}\right) \\ = \; & \frac{2}{(\mu+1)^3}\left(-\mu(\mu+2\mu_1-1)(\mu+\mu_1)\right. \\ & \left.\pm\left(\frac{\mu(\mu+2\mu_1-1)^2}{4(\mu_1+\mu)} - \frac{(2\mu+3\mu_1+\mu_1\mu)\mu_1(1+\mu)}{\mu+2\mu_1+\mu_1\mu}\right)\sqrt{K}\right). \end{aligned}$$

Using Eq. 34, we get r^2:

$$\begin{aligned} r^2 \; = \; & \frac{Y_{pq}^2 D' - B'}{A' - Y_{pq}^2 C'} \\ = \; & \frac{\mu}{2(\mu-\mu^2+2\mu_1)^2(\mu+\mu_1)(\mu+1)}\left(\mu+\mu_1 \pm \frac{1}{\mu}\sqrt{K}\right) \\ & \times\left(-\mu(\mu+2\mu_1-1)(\mu+\mu_1)\right. \\ & \left.\pm\left(\frac{\mu(\mu+2\mu_1-1)^2}{4(\mu+\mu_1)} - \frac{(2\mu+3\mu_1+\mu_1\mu)\mu_1(1+\mu)}{\mu+2\mu_1+\mu_1\mu}\right)\sqrt{K}\right). \end{aligned}$$

And expressing it as a function of the type $r^2 = F \pm G\sqrt{K}$, the average value is given by F, which gives

$$\begin{aligned} r_{avg}^2 \; = \; & \frac{\mu}{8(\mu-\mu^2+2\mu_1)^2(\mu+\mu_1)(\mu+1)} \\ & \times\left(-4\mu(\mu+2\mu_1-1)(\mu+\mu_1)^2 - \mu(\mu+2\mu_1-1)^2(\mu+2\mu_1+\mu_1\mu)\right. \\ & \left.+4(2\mu+3\mu_1+\mu_1\mu)\mu_1(1+\mu)(\mu+\mu_1)\right). \end{aligned}$$

By expanding the polynomial expression to μ and μ_1 between the large parentheses of this expression, we obtain

$$\begin{aligned} & -4(\mu^2+2\mu_1\mu-\mu)(\mu^2+2\mu_1\mu+\mu_1^2) \\ & -(\mu^2+2\mu_1\mu+\mu_1\mu^2)(\mu^2+4\mu_1^2+1+4\mu_1\mu-2\mu-4\mu_1) \\ & +4(2\mu_1\mu+3\mu_1^2+\mu_1^2\mu)(\mu^2+\mu+\mu_1\mu+\mu_1) \\ = \; & -5\mu^4 - 12\mu_1\mu^3 - 4\mu_1^2\mu^2 + 6\mu^3 + 23\mu_1\mu^2 + 32\mu_1^2\mu \\ & -\mu^2 - 2\mu_1\mu - \mu_1\mu^4 + 12\mu_1^3 \end{aligned}$$

This last expression can be factorized into

$$(-\mu^2+\mu+2\mu_1)(\mu_1\mu^2+6\mu_1^2+13\mu_1\mu+5\mu^2-\mu)$$

We therefore deduce the expression in simplified form of r_{avg}^2:

$$r_{avg}^2 = r_{opt}^2 = \frac{\mu(\mu_1\mu^2+6\mu_1^2+13\mu_1\mu+5\mu^2-\mu)}{8(\mu-\mu^2+2\mu_1)(\mu+\mu_1)(\mu+1)}$$

6.2 Annex B: Determination of optimal damping ratio r for P and R at equal height

We differentiate with respect to g^2 the 4 functions appearing in Eq. 15:

$$\begin{aligned} A \; &= \; 4f^2g^2(\mu+\mu_1)^2, \\ B \; &= \; \left(\mu_1 g^2 - (\mu+\mu_1)f^2\right)^2, \\ C \; &= \; 4f^2g^2\left((1+\mu)g^2-1\right)^2, \\ D \; &= \; \left(\mu f^2 g^2 - (g^2-1)(g^2-f^2)\right)^2, \end{aligned}$$

to get

$$\begin{aligned}
A' &= 4f^2(\mu+\mu_1)^2,\\
B' &= 2\mu_1\left(\mu_1 g^2-(\mu+\mu_1)f^2\right),\\
C' &= 4f^2((1+\mu)g^2-1)\left((1+\mu)g^2-1+2(1+\mu)g^2\right)\\
&= 4f^2((1+\mu)g^2-1)(3(1+\mu)g^2-1),\\
D' &= 2\left(\mu f^2 g^2-(g^2-1)(g^2-f^2)\right)(\mu f^2-2g^2+f^2+1)\\
&= \frac{2}{\mu+\mu_1}((1+\mu)g^2-1)\left(\mu_1 g^2-(\mu+\mu_1)f^2\right)\left((\mu+1)f^2+1-2g^2\right).
\end{aligned}$$

By replacing f by f_{opt} from Eq. 32 and g by $g_R = 1/(\sqrt{1-\mu_1})$, we calculate the expression $A' - Y_{pr}^2 C'$ at point R:

$$A' - Y_{pr}^2 C' = -8f_{opt}^2(\mu+\mu_1)(\mu+1).$$

Similarly, we calculate the expression $Y_{pr}^2 D'$ at the point R:

$$Y_{pr}^2 D' = \frac{2(2\mu+3\mu_1+\mu\mu_1)(5\mu\mu_1+\mu^2\mu_1-\mu+\mu^2+2\mu_1^2)}{(1-\mu_1)(\mu+1)^3}.$$

Finally, we calculate B' at point R:

$$B' = \frac{2\mu_1}{(1-\mu_1)(\mu+1)^2}(5\mu\mu_1+\mu^2\mu_1-\mu+\mu^2+2\mu_1^2).$$

This leads to $Y_{pr}^2 D' - B'$:

$$Y_{pr}^2 D' - B' = \frac{4}{(1-\mu_1)(\mu+1)^3}(5\mu\mu_1+\mu^2\mu_1-\mu+\mu^2+2\mu_1^2)(\mu+\mu_1).$$

By dividing the expressions obtained, we get r_R^2:

$$r_R^2 = -\frac{1}{2(\mu+1)^2(1-\mu-2\mu_1)}(5\mu\mu_1+\mu^2\mu_1-\mu+\mu^2+2\mu_1^2)(\mu+\mu_1).$$

We proceed in the same way by replacing f by f_{opt} from Eq. 32 and g by g_P from Eq. 31. We first get $A' - Y_{pr}^2 C'$ at point P:

$$A' - Y_{pr}^2 C' = 8f_{opt}^2(\mu+\mu_1)(1-\mu-2\mu_1).$$

Similarly, we calculate the expression $Y_{pr}^2 D'$ at point P:

$$Y_{pr}^2 D' = \frac{2\mu(1-\mu-2\mu_1)(2\mu+\mu_1-\mu\mu_1)}{(\mu+1)^3}.$$

Finally, we calculate B' at point P:

$$B' = -\frac{2\mu\mu_1(1-\mu-2\mu_1)}{(1-\mu_1)(\mu+1)^2}.$$

We deduce $Y_{pr}^2 D' - B'$:

$$Y_{pr}^2 D' - B' = \frac{4\mu(1-\mu-2\mu_1)}{(\mu+1)^3}(\mu+\mu_1).$$

By dividing the expressions obtained, we get r_P^2:

$$r_P^2 = \frac{\mu(1-\mu_1)}{2(\mu+1)(1-\mu-2\mu_1)}.$$

In analogy with the previous case (significant points P and Q), we define the square of the optimal damping by the average of the square of optimal damping at P and R, $r_{opt}^2 = \frac{1}{2}(r_R^2 + r_P^2)$. We obtain

$$r_{opt}^2 = \frac{\mu-3\mu\mu_1-\mu^2\mu_1-\mu_1^2}{2(1+\mu)^2(1-\mu-2\mu_1)}.$$